

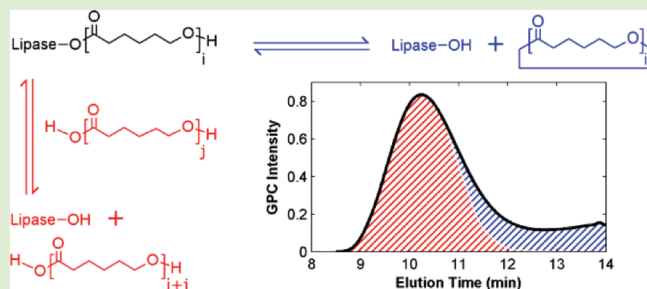
# Modeling Enzymatic Kinetic Pathways for Ring-Opening Lactone Polymerization

Peter M. Johnson,<sup>†,‡</sup> Santanu Kundu,<sup>†</sup> and Kathryn L. Beers<sup>†,\*</sup>

<sup>†</sup>Polymers Division, National Institute of Standards and Technology, Gaithersburg, Maryland 20899, United States

**S** Supporting Information

**ABSTRACT:** A unified kinetic pathway for the enzyme-catalyzed polymerization and degradation of poly( $\epsilon$ -caprolactone) was developed. This model tracks the complete distribution of individual chain lengths, both enzyme-bound and in solution, and successfully predicts monomer conversion and the molecular mass distribution as a function of reaction time. As compared to reported experimental data for polymerization reactions, modeled kinetics generate similar trends, with ring-opening rates and water concentration as key factors to controlling molecular mass distributions. Water is critically important by dictating the number of linear chains in solution, shifting the molecular mass distribution at which propagation and degradation equilibrate. For the enzymatic degradation of poly( $\epsilon$ -caprolactone), the final reaction product is also consistent with the equilibrium dictated by the propagation and degradation rates. When the modeling framework described here is used, further experiments can be designed to isolate key reaction steps and provide methods for improving the efficiency of enzyme polymerization.



## INTRODUCTION

Sustainable alternatives to current petroleum-based processes have become increasingly popular with the development and application of biobased raw materials and green synthesis routes.<sup>1,2</sup> In current polymer applications, renewable feedstocks are frequently used to complement or replace portions of current sources. Rapid innovation has generated a variety of novel renewable monomers and enzyme catalysts that provide routes to different polymer types, some with enhanced structural control. In the case of lipase-catalyzed polymerization of poly( $\epsilon$ -caprolactone) (PCL), previous work has shown milder processing conditions than standard heavy metal catalysts, which would reduce energy costs and reduce toxicity.<sup>3,4</sup> However, polymerization kinetic pathways have been difficult to predict fully, preventing the determination of selective amplification methods to create high molecular mass chains.<sup>5</sup>

When PCL is synthesized using an enzyme catalyst,  $\epsilon$ -caprolactone is ring opened by the enzyme and polymer is produced through secondary reaction steps.<sup>6–8</sup> This ring-opening step is well quantified, because the conformational change allows for the  $\epsilon$ -caprolactone consumption to be tracked using a variety of analytical techniques.<sup>9,10</sup> The end product, a complex molecular mass distribution that includes a large fraction of low molecular mass species, has also been characterized with gel permeation chromatography.<sup>11–15</sup> However, these two measurement techniques alone cannot fully explain the secondary reaction steps where ring opened  $\epsilon$ -caprolactone combines to form high molecular mass chains, nor do they provide sufficient insight into the

balance of pathways that produce the observed complex mass distributions. Previous studies have determined the influence of water in initiation and cyclic formation, molecular mass limitations at high  $\epsilon$ -caprolactone conversion, and enzymatic activity over time.<sup>15–19</sup> These studies have elucidated potential reaction steps when using an enzyme catalyst, but the complete framework has remained unclear.

In this work, we build a kinetic model that describes the catalytic kinetic pathways of *Candida antarctica* Lipase B enzyme with respect to the synthesis of PCL. This set of reactions successfully describes both enzymatic polymerization from  $\epsilon$ -caprolactone and enzymatic degradation of PCL. Although the general model was developed around this specific, well-studied system, the descriptors are general enough that the approach could be applied broadly, in principle, to other enzyme-catalyzed ring-opening polymerizations of polyesters that occur from similar transesterification reactions. By tracking every possible polymer chain, both enzyme bound and in solution, the full molecular mass distribution was tracked as a function of time.

Kinetic models have been successfully developed for a large number of polymerization reactions initiated from thermal, photochemical, or catalyst-mediated reaction mechanisms.<sup>20–25</sup> Previous approaches to modeling similar enzyme-catalyzed reactions used reactive group models or method of moments, which

**Received:** July 5, 2011

**Revised:** August 10, 2011

**Published:** August 11, 2011

described the need for both propagation and degradation reactions occurring simultaneously.<sup>26</sup> However, the model fails to represent the overall molecular mass distribution correctly because it cannot fully represent its complexity. In this model, the complete molecular mass distribution was tracked as a function of time. Model results were validated to both enzyme-catalyzed polymerization and degradation experiments, and the balances in the reaction equilibrium were studied in detail to validate key experimental observations. With a deeper understanding of the kinetic reactions available when using an enzyme catalyst, key reaction conditions can be described and studied in detail for future optimization of enzymatic synthesis routes.

## EXPERIMENTAL SECTION

**Materials.** Toluene and  $\epsilon$ -caprolactone were purchased from Sigma-Aldrich (Milwaukee, WI) and dried over 0.4 nm molecular sieves and anhydrous calcium hydride. For degradation experiments, toluene was saturated with water (wet toluene) by sonicating a solution of toluene with a droplet of water, then waiting 24 h before separating the immiscible fraction. Poly(methyl methacrylate) beads with immobilized *Candida antarctica* lipase B (Novozym N435) were obtained from Novozymes (Bagsvaerd, Denmark). N435 beads were sieved to obtain a particle distribution with a diameter of  $400 \mu\text{m} \pm 50 \mu\text{m}$  and were stored under vacuum until use. For this size distribution, N435 beads have an average of 10% enzyme by mass. PCL with an number average

relative molecular mass ( $M_n$ ) of 6000 g/mol (polydispersity = 4.9) produced in a microfluidic reactor using enzyme synthesis was used for degradation experiments.<sup>15</sup> A commercially produced PCL with  $\alpha$ - $\omega$  hydroxyl end groups ( $M_n = 10000$  g/mol, polystyrene equivalent) was purchased from Sigma Aldrich and was used as received. Equipment, instruments, or materials are identified in the paper in order to adequately specify the experimental details. Such identification does not imply recommendation by National Institute of Standards and Technology, nor does it imply the materials are necessarily the best available for the purpose.

**Experimental Design.** Both polymerization and degradation reactions were performed in an argon-purged 5 mL round-bottom flask, maintained at 70 °C and stirred at 60 rad/s. Water content was calculated for each component individually using a coulometric Karl Fischer water content apparatus (Mettler-Toledo C20, Columbus, OH) at room temperature. This measurement only quantifies free water available in solution, and any trapped or inaccessible water to the Karl Fischer reagents is not included. Water content and initial reaction conditions are given in Table 1. Polymerization experiments had an initial water concentration of 0.0213 mol/L; the concentration for degradation experiments was 0.0533 mol/L.

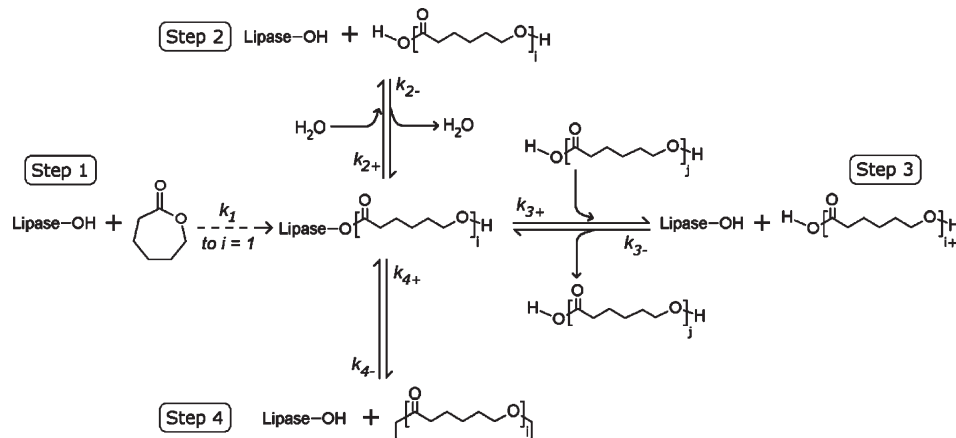
Gel permeation chromatography (GPC) and Raman spectroscopy were used to characterize reaction products. For GPC, a Waters system with three mixed bed columns (HR0.5, HR3, and HR4E, 5  $\mu\text{m}$  particle size) was run under conditions of 0.35 mL/min THF eluent at 30 °C and a sample size of 40  $\mu\text{L}$  injection volume, with a concentration of 5 mg/mL. A set of five narrow polydispersity polystyrene standards were used to calibrate the GPC system. The molecular masses reported here are for PCL molecular mass, converted from polystyrene equivalent masses to PCL molecular masses using the Mark–Houwink theory.<sup>27</sup> The parameters used were  $K_{\text{PS}} = 29.0 \times 10^{-5} \text{ dL/g}^{-1}$ ,  $K_{\text{PCL}} = 30.6 \times 10^{-5} \text{ dL/g}^{-1}$ ,  $a_{\text{PS}} = 0.634$ , and  $a_{\text{PCL}} = 0.70$ .<sup>27</sup> It is noted that Mark–Houwink calculations are less accurate for molecular mass chains below 1000 g/mol. The uncertainty in the measurement of polystyrene equivalent molecular mass is 10%.

For polymerization experiments, Raman spectroscopy was used to monitor the ring-opening of  $\epsilon$ -caprolactone.<sup>15,28</sup> Raman spectroscopy was collected with a Raman Systems (R3000HR) Raman spectrometer. Spectra were collected in situ using a fiber optic probe with a 5 mm focal depth and a 785 nm excitation wavelength laser. Spectra were collected for 20 s, with 110 s intervals between measurements. Ring-opening of  $\epsilon$ -caprolactone was monitored from the ring breathing peak area at  $696 \text{ cm}^{-1}$  normalized to a

**Table 1. Water Content for Each Reaction Component and Initial Conditions for Polymerization and Degradation Reactions**

material	mass fraction ( $\times 10^{-6}$ )	initial conditions	
		polymerization	degradation
toluene	$40 \pm 4$	2 mL	0 mL
$\epsilon$ -caprolactone	$40 \pm 4$	1 mL	0 mL
wet toluene	$450 \pm 7$	0 mL	2 mL
PCL	$1030 \pm 15$	0 mL	1 mL
N435 beads	$10200 \pm 300$	100 mg	100 mg

**Scheme 1. Modeled Kinetic Reactions in Enzyme-Mediated Poly( $\epsilon$ -caprolactone) Synthesis<sup>a</sup>**



<sup>a</sup> Subscripts on kinetic rate parameters denote the reaction step number. Positive subscripts are reactions with enzyme-activated PCL chains; negative subscripts are reactions with free enzyme sites.

**Table 2. Kinetic Rate Constants Used in the Complete Distribution Model<sup>a</sup>**

chain length dependence	kinetic rate parameter ( $k_0$ )
$k_1 = k_{10}$	150 L/mol/s
$k_{2+} = k_{2+,0}$	36000 L/mol/s
$k_{2-} = k_{2-,0} j^{-0.5}$	4000 L/mol/s
$k_{3+} = k_{3+,0} j^{-0.5}$	3000 L/mol/s
$k_{3-} = k_{3-,0} j^{-0.5}$	3000 L/mol/s
$k_{4+} = k_{4+,0} i^{-1.5}$	1500 1/s
$k_{4-} = k_{4-,0} j^{-0.5}$	4000 L/mol/s

<sup>a</sup>The chain length dependence is also shown, where  $i$  is the number of repeat units in an enzyme-activated polymer chain (EP<sub>*i*</sub>) and  $j$  is the number of repeat units in a linear or cyclic chain in solution.

toluene peak at 1002 cm<sup>-1</sup>. All samples were measured in triplicate, with error shown as standard deviations when present.

**Kinetic Reactions.** The kinetic model is based on the reaction pathways proposed by Mei et al., reorganized into four reaction steps (Scheme 1).<sup>10</sup> These four reaction steps all require enzyme to be present and include the reaction for  $\epsilon$ -caprolactone ring-opening, enzyme and polymer chain interactions with water, chain propagation or degradation, and cyclic formation. When modeling polymerization, initial conditions consist of three reaction species: active enzyme sites (E), water (H<sub>2</sub>O), and  $\epsilon$ -caprolactone ( $\epsilon$ CL). As the polymerization proceeds, three PCL chain configurations must be considered. The first possible polymer chain type, an enzyme-activated polymer chain (EP<sub>*i*</sub>), is a PCL chain that is attached to the lipase at the active site. The second chain category, a linear chain (P<sub>*i*</sub>), is an unattached PCL chain in solution, containing one hydroxyl and one carboxylic acid end group. The third chain type, a cyclic chain (C<sub>*i*</sub>), is a PCL chain in solution that has formed a ring from intermolecular backbiting of an enzyme-activated polymer chain. The equilibrium between chain configurations and the enzyme-mediated ring-opening of  $\epsilon$ CL form the kinetic pathways and are shown in Scheme 1.

Step 1 in the reaction pathway is the enzyme-mediated ring-opening of  $\epsilon$ CL (kinetic rate parameter:  $k_1$ ). This reaction is considered irreversible, as ring strain should prevent the ring from reforming. The product of this reaction step is an enzyme-activated polymer chain of length  $i = 1$ , with an ester bond linkage at the active enzyme site. Previous experimental studies have shown this step has first order dependence with respect to  $\epsilon$ CL.<sup>6,10,15</sup>

Steps 2 and 3 describe the equilibrium between enzyme-activated polymer chains and linear chains in solution. In the forward reaction ( $k_{2+}$ ) of step 2, water is consumed to break the ester bond formed between the enzyme and PCL chain, forming a linear PCL chain and an active enzyme. In the backward reaction of step 2 ( $k_{2-}$ ), an ester bond is formed at the enzyme active site with the carboxylic acid end group on a linear chain, generating water. In this model, only water can create PCL linear chains in solution, and polymerization would not occur if all water was removed. Other initiators, such as alcohols, will initiate the reaction and prevent cyclic formation through end-capping.<sup>29</sup>

In the forward reaction ( $k_{3+}$ ) of step 3, enzymatic polycondensation occurs when enzyme-activated chains react with the hydroxyl group at the end of a linear chain in solution, forming an ester bond between the two PCL chains. This reaction results in a high molecular mass chain and an active enzyme site. Propagation of the enzyme-activated monomer is included in this reaction when  $i = 1$ . In the reverse reaction of step 3 ( $k_{3-}$ ), the enzymatic degradation occurs when the active enzyme site cleaves an ester bond at a random position of a PCL chain, reforming the ester bond with the enzyme active site. This results in a lower molecular mass linear chain and an enzyme activated polymer chain.

Step 4 describes the equilibrium between enzyme activated chains and cyclic chains in solution. In the forward step ( $k_{4+}$ ), cyclic formation occurs when the bound PCL chain backbites on itself at the active site, forming an ester bond with itself to form a cyclic chain. The enzyme active site is regenerated. The reverse reaction ( $k_{4-}$ ) is the ring-opening of a cyclic chain, mechanistically similar to step 1, although with a larger ring. This ring-opening changes the chain conformation to an enzyme-activated polymer chain.

All modeled reactions require either enzyme-activated polymer chains or an active enzyme site. Additional reactions, such as hydrolysis reactions, were ignored due to the reaction rate being orders of magnitude slower than enzymatic reactions when performed without other catalysts. In control experiments, reactant solutions that contain no enzyme at 70 °C were unchanged over 8 h. Enzyme activity is assumed to remain constant over the reaction lifetime.

**Modeling and Kinetic Rates.** Because the molecular mass distribution for this reaction produces a nonuniform distribution, every chain length and chain configuration was modeled individually. This set of chain lengths formed the complete molecular mass distribution. Kinetic parameters, along with chain length dependent weighting, are given in Table 2. In systems where the entire molecular mass distribution is modeled, the kinetic rate parameters are commonly combined with molecular mass dependence terms, which capture the change in the kinetic rate as a function of chain length. In this system, molecular mass dependence was considered only for polymer chains reacting with a free enzyme site or an enzyme-activated polymer chain.

For bimolecular reactions involving a polymer in solution, a kinetic rate parameter weighting function is  $i^{-1/2}$ , where  $i$  is the number of units in the polymer chain.<sup>30</sup> This weighting function is derived from diffusion limited kinetic parameters. Detailed explanations of kinetic rate parameter dependencies are described in the Supporting Information, including the assumptions and derivations for weighting calculations and additional steric effects. Briefly, the main assumptions are imposing a homogeneous system model and setting enzyme diffusion in chain length dependence calculations to zero. This assumption removed any effects from bead dimensions, pore size exclusion, or enzyme availability from the model, but these simplifications were necessary for simplifying the model to an initial computationally tenable equation set, because the presence of the enzyme–polymer support would require a heterogeneous model and a significant expansion of adjustable parameters.

The chain length dependence term is generally valid in solutions where specific moieties on two large species must react, in this case, a PCL chain end to a specific region of the enzyme. Additional steric hindrance from the polymer chain attached to the enzyme is ignored, because the enzyme is immobilized to the bead. For cyclic formation, the chain length dependence for ring formation based on the Jacobson–Stockmayer theory was used,  $i^{-1.5}$ , because the chain end and reactive species must be in the same physical space while constrained by a random Gaussian chain. Cyclic formation is unimolecular. Chain scission during degradation was assumed to be equally probable for every ester bond on the chain.

The kinetic rate parameters described here were found using factorial searches. The only kinetic parameter with a well-defined rate constant was the ring-opening step ( $k_1$ ), because this reaction was monitored in this work and has been reported on in literature. The initial predicted kinetic parameters were chosen to force the rate-limiting step to be the ring-opening reaction. Factorial searches were then performed using this initial condition as a center point. Model results determined that kinetic parameters could encompass a small range of valid values to produce an  $\epsilon$ CL consumption rate and a molecular mass distribution with a large fraction of cyclic oligomers consistent with polymerization experiments. Degradation experiments were not used to optimize kinetic parameters, instead serving as experiments to check the validity of the chosen kinetic

parameters. A full optimization of the kinetic parameters could not be performed due to the interrelated reaction pathways, because all three chain configurations exist in equilibrium. To decouple all kinetic rate parameters, linear and cyclic chain concentrations would need to be measured individually. Complex experimental designs or improved detection methods would be required to isolate individual rate parameters.

With the enzyme catalysis reaction pathway currently defined, ordinary differential equations were written for every species in the solution. All reactions were considered first order to each reaction component, and concentrations are based on the molecular mass of the PCL chain. Beginning with the simplest rate equations,  $\epsilon$ CL has a single reaction that is the enzyme-catalyzed ring-opening. Water and cyclic PCL chains are only included in a single equilibrium step. The reaction rate equations for these components were defined as

$$\frac{d[\epsilon\text{CL}]}{dt} = -k_1[\epsilon\text{CL}][E] \quad (1)$$

$$\frac{d[\text{H}_2\text{O}]}{dt} = -k_{2+} \sum_i [\text{EP}_i][\text{H}_2\text{O}] + \sum_j k_{2-}[P_j][E] \quad (2)$$

$$\frac{d[C_i]}{dt} = k_{4+}[E] - k_{4-}[C_i][E] \quad (3)$$

using the definitions for kinetic rate parameters given in Scheme 1 and Table 2. The concentration of PCL chains is based on the molecular mass of the polymer chain. Cyclic chains are considered only for chains between two and 175 repeat units. Chains greater than 175 repeat units were assumed to have minimal cyclic chain formation and reaction rates were set to zero. With these rates defined, the rate of change for free enzyme sites can be defined as

$$\begin{aligned} \frac{d[E]}{dt} = & -\frac{d[\epsilon\text{CL}]}{dt} - \frac{d[\text{H}_2\text{O}]}{dt} \\ & + \sum_i \sum_j k_{3+}[\text{EP}_i][P_j] - \sum_j k_{3-}[P_j][E] + \sum_m \frac{d[C_m]}{dt} \end{aligned} \quad (4)$$

where  $m = 2-175$ . Free enzyme sites are either generated or occupied in each reaction step, and this reaction rate demonstrates the convoluted nature of the reaction pathway. The free enzyme concentration is not solely dependent on a single rate parameter.

Both linear and enzyme bound chains have similar complexity. For enzyme-activated polymer chains, different chain lengths require additional reactions to be included. Three different reaction rates are needed and are defined as follows

$$R_{2i} = -k_{2+}[\text{EP}_i][\text{H}_2\text{O}] + k_{2-}[E][P_i] \quad (5)$$

$$\frac{d[\text{EP}_1]}{dt} = -\frac{d[\epsilon\text{CL}]}{dt} + R_{2i} + \sum_{m=2} k_{3-} \frac{[P_m]}{m-1} [E] \quad (6)$$

$$\left. \frac{d[\text{EP}_i]}{dt} \right|_2^{175} = -\frac{d[C_i]}{dt} + R_{2i} - \sum_j k_{3+}[\text{EP}_i][P_j] + \sum_{m=i+1} k_{3-} \frac{[P_m]}{m-1} [E] \quad (7)$$

$$\left. \frac{d[\text{EP}_i]}{dt} \right|_{176}^{1000} = R_{2i} - \sum_j k_{3+}[\text{EP}_i][P_j] + \sum_{m=i+1} k_{3-} \frac{[P_m]}{m-1} [E] \quad (8)$$

All reaction rates for enzyme-activated chains include steps 2 and 3, but the ring-opening rate chains of length  $i = 1$  and cyclic reactions were added for chains from 2 to 175 units in length. Degradation reactions were summed over all chains of greater size, and the equal probability for chain scission was included. For a chain of length  $m$ ,  $m - 1$  ester bonds

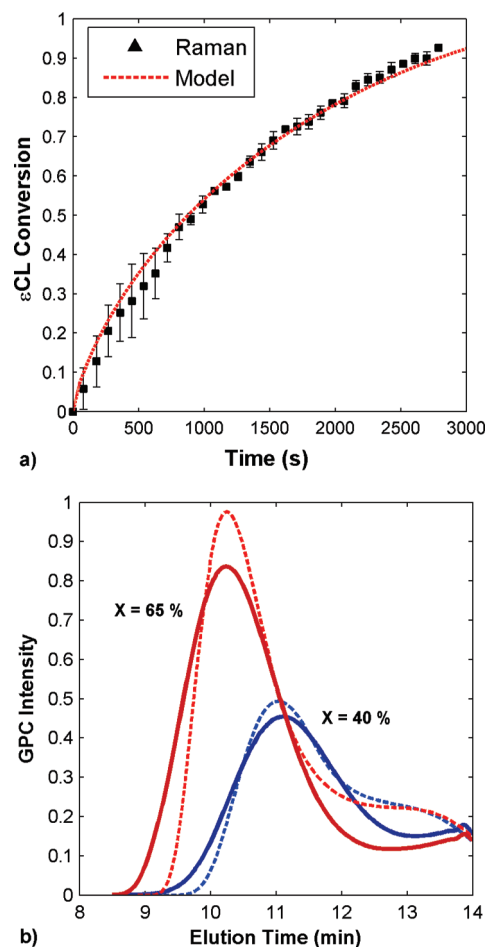


**Figure 1.** (a) Comparison of experimental (■) and model (---) results for  $\epsilon$ CL ring-opening conversion. (b) Experimental (---) and modeled (—) GPC traces for molecular mass distribution at 40% (blue) and 65% (red) conversion.

could be cleaved with a uniform probability of  $1/(m - 1)$ . Linear polymer chains were both consumed and created by the propagation/degradation reactions in step 3. The reaction rate for a linear PCL chain of length  $i$  in solution is given as

$$\begin{aligned} \frac{d[P_i]}{dt} = & -R_{2i} - \sum_j k_{3+}[\text{EP}_i][P_j] - k_{3-}[E][P_i] \\ & + \sum_{m=j+1} k_{3-} \frac{[P_m]}{m-1} [E] + \sum_{g=1}^{j-1} k_{3+}[\text{EP}_{j-g}][P_g] \end{aligned} \quad (9)$$

For linear chains in solution, reaction terms from step 2 are included with opposite signs as compared to the enzyme activated polymer chains. Terms creating and consuming chains for both the forward and backward reactions of step 3 are included. For a linear polymer chain of length  $i$ , propagation of lower molecular mass species would create this chain, while the chain would be consumed during propagation to higher molecular mass polymer. In degradation reactions, the same effect applies, except the chain is consumed to create lower molecular mass chains and created from the degradation of higher molecular mass chains.

The kinetic model was developed and solved in MATLAB with an ordinary differential equation (ODE) solver and a maximum relative molecular mass of 228000 or 114000 g/mol ( $i = 2000$  or 1000). Maximum values were much larger than necessary to capture all polycondensation events and prevent discontinuities in the model. Model

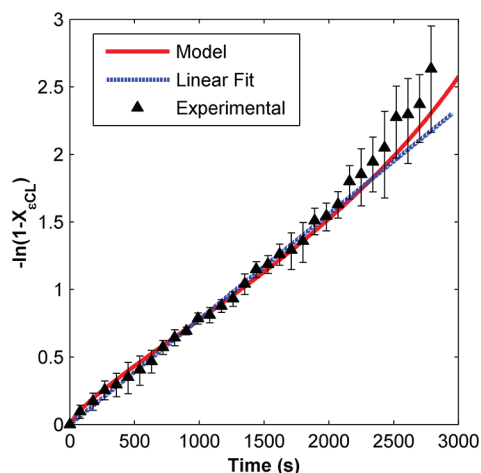


**Figure 2.** First order model fit vs experimental and kinetic model results.

error tolerances, species balances, and initial condition matrices are described in further detail in the Supporting Information. Initial concentrations were calculated from Table 1. Models for polymerization reactions were run for a simulated reaction time of 3000 s, while degradation reactions were modeled for 72000 s. The largest expected chain in the system can be set to a relatively low enough number due to the constraints of the kinetic pathway, providing reasonable computational requirements. Kinetic parameters in Table 2 were used for all modeling experiments.

## RESULTS

**Polymerization Kinetics.** Using the kinetic model described above, the molecular mass distribution for different polymerization reaction conditions was simulated. With the model output, the  $\epsilon$ CL ring-opening conversion and molecular mass distribution could be calculated for every time step. Comparison of the model results to experimental data is shown in Figure 1.

The ring-opening kinetics of  $\epsilon$ CL was matched to within error for the entire range of conversion shown. The molecular mass distribution for the kinetic model also shows a distribution similar to experimental results. The model results retain the high concentration of low molecular mass species throughout the polymerization. The molecular mass distribution, as indicated by the GPC trace, is similar but not equivalent, which is likely caused by the translation of model results to GPC equivalent data and potentially improved optimization of kinetic parameters. In particular, the cyclic chains elute at different speeds than linear chains.<sup>31</sup> When the molecular mass distribution from the model is used, the number average relative molecular mass,  $M_n$ , reaches a plateau at high conversion.<sup>10,15</sup> Figures showing  $M_n$  as a function of conversion, polymer chain concentration, and free enzyme concentration versus time are provided in the Supporting Information. Within the kinetic pathways described here, this effect is caused by the equilibrium between degradation and propagation. Without additional enzyme-activated monomer, reactions in step 3 should equilibrate, and the molecular mass should plateau. In addition, the cyclic reactions from step 4 are required to produce low molecular mass species, which persist throughout the reaction. These polymerization products cause deleterious effects to the resulting polymer, because low molecular mass species act as plasticizers.

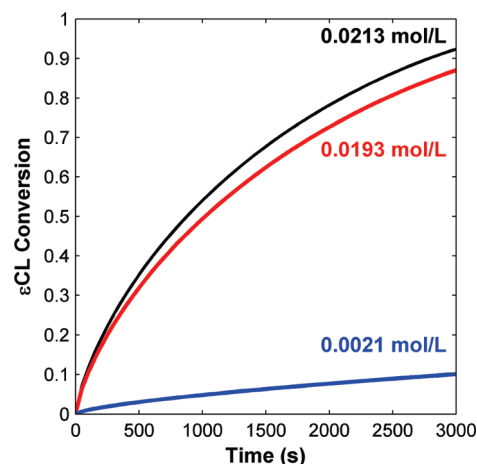


**Figure 3.** Modeled ring-opening conversion using standard initial conditions ( $[\text{H}_2\text{O}]_0 = 0.0213 \text{ mol/L}$ ) and two reduced water conditions. Reduced water conditions were calculated from including only water associated either with the enzyme bead (0.0193 mol/L; red) or the toluene/ $\epsilon$ CL solution (0.0021 mol/L; blue).

The ring-opening kinetic reaction rate appears first order to  $\epsilon$ CL frequently in the literature, assuming active enzyme concentrations remain constant at all times.<sup>10,15</sup> In the case of the results in Figure 1a, conversion ( $X_{\epsilon\text{CL}}$ ) results from the model and experimental data show good agreement, even though the enzyme concentration is allowed to vary. For first-order reactions, a plot of  $-\ln(1 - X_{\epsilon\text{CL}})$  versus reaction time should yield a straight line (Figure 2).

The ring-opening reaction rate yields a figure similar to a first order dependence. This apparent first order dependence was due to the free enzyme concentration remaining nearly constant over the monitored reaction time. Deviations at long times are caused by the reduced  $\epsilon$ CL concentration at high conversion. For most of the reaction, any other forward step that generates a free enzyme site has a high probability to react via step 1 into an enzyme-activated monomer,  $\text{EP}_1$ . When the  $\epsilon$ CL concentration is sufficiently reduced, the other equilibrium steps begin to compete for free enzyme sites. The reduction in  $\text{EP}_1$  at high conversion also means that polycondensation events will increase as the enzyme activated chains begin to increase in molecular mass. Literature reports have shown the recovery of water at high  $\epsilon$ CL conversion, also suggesting polycondensation events become more significant at higher conversion.<sup>18</sup> These effects are consistent with the kinetic pathway described here.

**Influence of Water.** While the ring-opening reaction is important to understanding the dominant reaction steps as a function of conversion, understanding the development of the molecular mass distribution is critical to developing better control of the end polymer and improving the process. The molecular mass distribution is controlled by the rest of the reaction pathway. Of the three initial components, water ( $[\text{H}_2\text{O}]_0 = 0.0213 \text{ mol/L}$ ) is a key factor, acting as the initiator and enabling degradation. Because the model allows for rapid analysis of the different initial conditions, the water concentration was varied. The initial water conditions were changed as if all trace water was removed from different components in the system through a prior processing step. Two initial water concentrations were considered, one where all freely accessible water was removed from the enzyme beads ( $[\text{H}_2\text{O}]_0 = 0.0021 \text{ mol/L}$ ) and one where all trace water

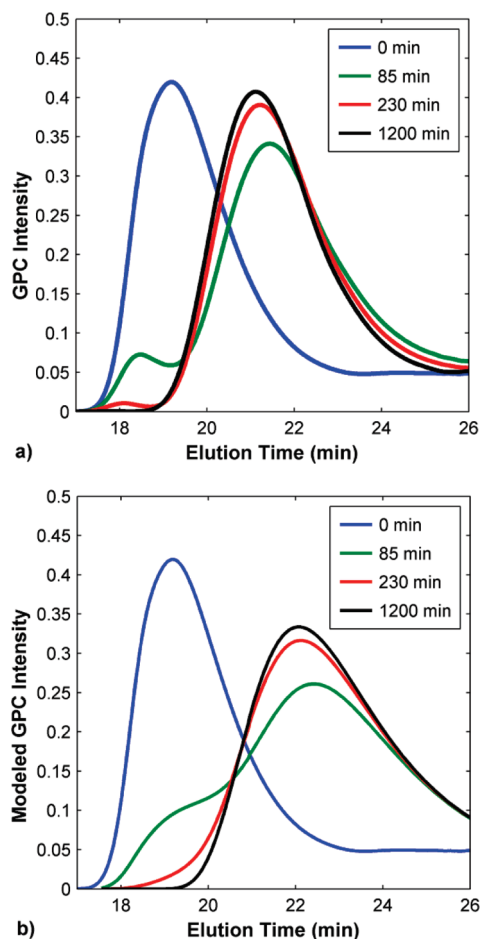


**Figure 4.** (a) GPC of degradation experiments at different reaction times. (b) Modeled GPC for similar initial molecular mass distribution, with the high molecular mass shoulder present in both the experimental and model results.

was removed from  $\epsilon$ CL and toluene ( $[\text{H}_2\text{O}]_0 = 0.0192 \text{ mol/L}$ ). While these water concentrations are idealized by discounting water affinity between the three components, they demonstrate potential effects of removing water from the reaction. These results are shown in Figure 3.

In both cases, the reduction of water decreases the ring-opening rate. However, a small reduction in water concentration, such as from the removal of all water from toluene and  $\epsilon$ CL, has a minor effect on the modeled  $\epsilon$ CL conversion. For the case where the N435 beads contain no water, the large reduction in the initial water concentration caused a significant reduction in the modeled  $\epsilon$ CL conversion. Because nearly all of the water is consumed during polymerization, the number of chains in the system is strongly dependent on the initial water concentration. With a lower linear PCL chain concentration, there are not enough chains for propagation. By slowing propagation, enzyme sites remain occupied for longer times, and the ring-opening rate is reduced. All four steps influence each other throughout the reaction, water concentration only directly impacts step 2, but indirectly impacts the rest of the kinetic pathway due to its control over the number of polymer chains in solution.

**Polymer Degradation.** Enzymatic degradation of PCL could also be performed, only requiring a switch from  $\epsilon$ CL to PCL as a starting material. This change causes a significant shift in the

kinetic pathway, since the ring-opening kinetic step is no longer active, leaving only chain equilibrium reactions. To shift the PCL molecular mass significantly, additional water is needed, so dry toluene was replaced with wet toluene. Degradation from enzyme polymerized PCL was monitored with aliquots for GPC at 0, 85, 230, and 1200 min. Initial water conditions are found in Table 1. Experimental results are shown in Figure 4a, with corresponding predicted GPC traces from the model molecular mass distribution in Figure 4b.

In Figure 4, a clear high molecular mass shoulder is evident in both the experimental results and the polymerization model. In addition, the low molecular mass peak shifts back to a slightly higher molecular mass with increased degradation time. These experimental results can be described by the kinetic pathway. In degradation, the equilibrium between water concentration and the number of free linear chains is out of balance initially. As mentioned previously, a higher water concentration should decrease the average molecular mass, since more linear chains exist in solution as the water concentration increases. The key factor for enzymatic degradation is that every degradation reaction requires a free enzyme site. Initially, the water concentration and number of linear PCL chains favor additional linear chains in solution to balance the step 2 equilibrium. Degradation in step 3 occupies an enzyme active site, before the enzyme activated PCL chain is quickly released, consuming water and regenerating free enzyme. When the linear chain and water concentration equilibrate, the dominant driving force shifts to the other available reactions. The initial water concentration is not high enough to consume all high molecular mass chains, so the rest of the high molecular mass chains degrade slowly, as seen in GPC. These remaining linear chains in solution degrade at a slower rate as the molecular mass distribution equilibrates to a value consistent for the number of linear chains available. Because equilibrium between degradation and propagation is always present, excess water would be required to reduce PCL to a ring-opened monomer unit. Excess water is defined as accessible water above the concentration dictated by the equilibrium in Step 2 between linear PCL chains and water. Over 20% of the initial water concentration remained in the degradation model once the molecular mass distribution reached equilibrium.

While the trends are similar in the experimental results and the model, the molecular mass distribution shifts to smaller chain lengths than expected. Because the initial conditions define PCL as only linear polymer chains, the cyclic chains that should be accounted for in an enzymatically synthesized product are not. However, the distribution of cyclic and linear chains cannot be distinguished in conventional GPC analysis, and a distribution inserted into the initial conditions could bias further kinetic and mass distribution optimization. In the Supporting Information,  $M_n$  versus reaction time and experimental GPC results from degradation experiments and model predictions for a commercially provided PCL are shown. Degradation occurs, but differences arise due to changes in end group functionality as compared to enzymatic PCL.

## CONCLUSIONS

By discretely modeling every PCL chain length and chain type, we have developed a model which describes the enzymatic pathways which govern the polymerization and degradation of poly( $\epsilon$ -caprolactone). This model describes the equilibrium

reactions between the enzyme-activated chains, linear chains, and cyclic chains, which create PCL from ring-opened  $\epsilon$ CL and the enzymatic degradation of PCL. For polymerization, the model accurately described both the ring-opening rate and resulting molecular mass distribution as a function of time. Removing trace water in initial reaction components caused the reaction rate to shift due to the decrease of the water concentration, which limits the number of linear chains that can propagate. Enzymatic degradation experiments use the same kinetic pathways to form lower molecular mass products, and the same kinetic pathway modeled the short time high molecular mass shoulder. Degradation initially proceeds quickly as high water concentrations increase the availability of free enzyme sites to degrade chains. But once the water is consumed, the degradation switches to a much slower mechanism to degrade high molecular mass species completely. Since the reaction pathway is dominated by equilibrium reactions, optimization of the kinetic pathways must account for this effect and enable development of new reaction designs which mitigate unwanted side reactions. Although the model is applied to  $\epsilon$ CL as a model system in this treatment, the principles and equations are general such that they should apply to ring-opening polyester synthesis through enzyme catalyzed transesterification, such as lactones, lactams, and cyclic carbonates.

## ■ ASSOCIATED CONTENT

**S Supporting Information.** Expanded details on kinetic rate parameter modeling with model error analysis, number average and weight average relative molecular mass, enzyme concentration, and PCL chain concentration for polymerization experiments. Model and experimental degradation results using commercial PCL. This material is available free of charge via the Internet at <http://pubs.acs.org>.

## ■ AUTHOR INFORMATION

### Corresponding Author

\*E-mail: [kathryn.beers@nist.gov](mailto:kathryn.beers@nist.gov).

### Present Addresses

<sup>†</sup>Department of Materials Science and Engineering, University of Maryland, College Park, MD 20742.

## ■ ACKNOWLEDGMENT

We would like to thank Charles Guttman, William Wallace, and Kathleen Flynn for their helpful discussions. We would also like to thank Atul Bhangale for help with Raman monomer conversion calibration.

## ■ REFERENCES

- (1) Kobayashi, S.; Makino, A. *Chem. Rev.* **2009**, *109*, 5288–5353.
- (2) Beach, E. S.; Cui, Z.; Anastas, P. T. *Energy Environ. Sci.* **2009**, *2*, 1038–1049.
- (3) Gross, R. A.; Kumar, A.; Kalra, B. *Chem. Rev.* **2001**, *101*, 2097–2124.
- (4) Labet, M.; Thielemans, W. *Chem. Soc. Rev.* **2009**, *38*, 3484–3504.
- (5) Kobayashi, S. *Macromol. Rapid Commun.* **2009**, *30*, 237–266.
- (6) Kumar, A.; Gross, R. A. *Biomacromolecules* **2000**, *1*, 133–138.
- (7) Mei, Y.; Kumar, A.; Gross, R. A. *Macromolecules* **2002**, *35*, 5444–5448.

- (8) Kobayashi, S.; Takeya, K.; Suda, S.; Uyama, H. *Macromol. Chem. Phys.* **1998**, *199*, 1729–1736.
- (9) Chen, B.; Miller, E. M.; Miller, L.; Maikner, J. J.; Gross, R. A. *Langmuir* **2007**, *23*, 1381–1387.
- (10) Mei, Y.; Kumar, A.; Gross, R. *Macromolecules* **2003**, *36*, 5530–5536.
- (11) Xiao, Y.; Takwa, M.; Hult, K.; Koning, C. E.; Heise, A.; Martinelle, M. *Macromol. Biosci.* **2009**, *9*, 713–720.
- (12) van der Meulen, I.; de Geus, M.; Antheunis, H.; Deumens, R.; Joosten, E. A. J.; Koning, C. E.; Heise, A. *Biomacromolecules* **2008**, *9*, 3404–3410.
- (13) Sivalingam, G.; Karthik, R.; Madras, G. *J. Anal. Appl. Pyrolysis* **2003**, *70*, 631–647.
- (14) Sivalingam, G.; Chattopadhyay, S.; Madras, G. *Polym. Degrad. Stab.* **2003**, *79*, 413–418.
- (15) Kundu, S.; Bhangale, A. S.; Wallace, W. E.; Flynn, K. M.; Guttman, C. M.; Gross, R. A.; Beers, K. L. *J. Am. Chem. Soc.* **2011**, *133*, 6006–6011.
- (16) Bankova, M.; Kumar, A.; Impallomeni, G.; Ballistreri, A.; Gross, R. A. *Macromolecules* **2002**, *35*, 6858–6866.
- (17) Deng, F.; Bisht, K. S.; Gross, R. A.; Kaplan, D. L. *Macromolecules* **1999**, *32*, 5159–5161.
- (18) Dong, H.; Cao, S.-G.; Li, Z.-Q.; Han, S.-P.; You, D.-L.; Shen, J.-C. *J. Polym. Sci., Part A: Polym. Chem.* **1999**, *37*, 1265–1275.
- (19) Dong, H.; Wang, H.-D.; Cao, S.-G.; Shen, J.-C. *Biotechnol. Lett.* **1998**, *20*, 905–908.
- (20) Buback, M.; Junkers, T. *Macromol. Chem. Phys.* **2006**, *207*, 1640–1650.
- (21) Buback, M.; Egorov, M.; Gilbert, R. G.; Kaminsky, V.; Olaj, O. F.; Russell, G. T.; Vana, P.; Zifferer, G. *Macromol. Chem. Phys.* **2002**, *203*, 2570–2582.
- (22) Yu, Y. C.; Storti, G.; Morbidelli, M. *Macromolecules* **2009**, *42*, 8187–8197.
- (23) Johnson, P. M.; Stansbury, J. W.; Bowman, C. N. *Macromolecules* **2008**, *41*, 230–237.
- (24) Thickett, S. C.; Gilbert, R. G. *Polymer* **2007**, *48*, 6965–6991.
- (25) Litmanovich, A. D.; Plate, N. A.; Kudryavtsev, Y. V. *Prog. Polym. Sci.* **2002**, *27*, 915–970.
- (26) Sivalingam, G.; Madras, G. *Biomacromolecules* **2004**, *5*, 603–609.
- (27) Huang, Y.; Xu, Z. D.; Huang, Y. P.; Ma, D. Z.; Yang, J. C.; Mays, J. W. *Int. J. Polym. Anal. Character.* **2003**, *8*, 383–394.
- (28) Khan, J. H.; Schue, F.; George, G. A. *Polym. Int.* **2010**, *59*, 1506–1513.
- (29) Peeters, J. W.; van Leeuwen, O.; Palmans, A. R. A.; Meijer, E. W. *Macromolecules* **2005**, *38*, 5587–5592.
- (30) Benson, S. W.; North, A. M. *J. Am. Chem. Soc.* **1962**, *84*, 935–940.
- (31) Hoskins, J. N.; Grayson, S. M. *Macromolecules* **2009**, *42*, 6406–6413.